

Elsevier Editorial System(tm) for
Neurocomputing
Manuscript Draft

Manuscript Number: NEUCOM-D-13-01780R1

Title: Hybrid Neural Network Predictive-Wavelet Image Compression System

Article Type: SI: ICIC 2013

Keywords: Neural Network, predictive coding, image compression,
quantisation

Corresponding Author: Dr. Abir Hussain,

Corresponding Author's Institution:

First Author: Abir Hussain

Order of Authors: Abir Hussain; Dhiya Al Jumeily, PhD; Naeem Radi, PhD;
Paulo Lisboa , PhD

Abstract: This paper considers a novel image compression technique called Hybrid Predictive Wavelet coding. The new proposed technique combines the properties of predictive coding and discrete Wavelet coding. In contrast to JPEG2000, the image data values are pre-processed using predictive coding to remove inter-pixel redundancy. The error values, which are the difference between the original and the predicted values, are discrete wavelet coding transformed. In this case, a nonlinear neural network predictor is utilised in the predictive coding system. The simulation results indicated that the proposed technique can achieve good compressed images at high decomposition levels in comparison to JPEG2000.

The authors would like to thank the reviewers for their constructive comments which have certainly improved the quality of the paper significantly.

Reviewer #1: - The paper proposes an image compression system based on neural networks. I found the paper well written, technically sound and with clear focus.

- The authors have provided a good study of related techniques and the proposed approach is well motivated. I have two minor comments to improve the experimental part of the paper further.

The authors would like to thank the reviewer for his/her encouraging comment.

- The first comment concerns the quantitative results. I suggest that the authors study the statistical significance of the results as compared to other approaches. Actually it will be helpful to test if the difference between the proposed approach and comparable approaches is statistically significant.

To check the statistical significance between the proposed HNNPWA and JPEG 2000 techniques, the authors performed a paired t-test based on the Absolute value of the error image. The calculated t-values showed that the proposed technique outperforms JPEG2000 with $\alpha = 5\%$ significance level for a one-tailed test at decomposition levels 4, 5 and 6. The t-test indicated that there is no significant difference between the two image compression techniques at decomposition level 3.

As it can be noted from Figure 8, at decomposition levels 1, 2 and 3, the visual quality of the reconstructed images for the proposed HPNNA and JPEG2000 is very good and it is not easy to notice the difference between the original image and the constructed image for both systems.

- The comparison is mainly based on the PSNR which is the most widely used approach. Are there other measures that can be used to emphasize further the advantages of the proposed approach.

For all the experiments, the authors have added the mean absolute value of the error as another quality measure.

- Finally, the conclusion could be improved further by adding more analysis and discussions that could be devoted to explaining the main problems that could be related to the application of the proposed approach.

The conclusion section was expanded and the problem of the application of the proposed system was mentioned as requested by the reviewer.

Reviewer #2: The quality of written presentation demonstrates a good standard of writing, coherency and logical flow. However it contains some minor mistakes and I hope that these comments and suggestions are useful and can help the authors improve their scientific work and/or presentation.

- 1) Line spacing - in some parts of the paper line spacing was not addressed carefully (spacing between paragraphs)

The authors have addressed the line spacing in the paper as requested by the reviewer

- 2) I would suggest the authors to put equation number for every equation in the paper.

The authors have included numbers to all equations.

- 3) Section 1: Introduction- 2nd last para- "In the proposed work, the amount of... original image data" - please rephrase, it is confusing.

This paragraph was replaced by the following:

In the proposed work, Differential Pulse Code Modulation (DPCM) or Predictive Coding was used to remove inter-pixel redundancy and produce Prediction Errors (PE) which has smaller entropy than the original image data.

4) Figure 4 is unclear.

Figure 4 was replaced with clearer structure to the NARX neural network

5) Figure 7 : what are LL, HL, HH?

Explanation about LL, HL, HH were included in the figure where:

HL: High frequency band with Low pass filters

HH: High frequency band with High pass filters

LL: Low frequency band with Low pass filters

LH: Low frequency band with High pass filters

6) Section 5.1 - 2nd last para- please rearrange the paragraph.

This paragraph was arranged as follows:

These results indicated that the FLNN has achieved better results in comparison with the NARX and the MLP predictors. Hence, functional link neural network predictor was utilised in the proposed HNNPWA image compression system.

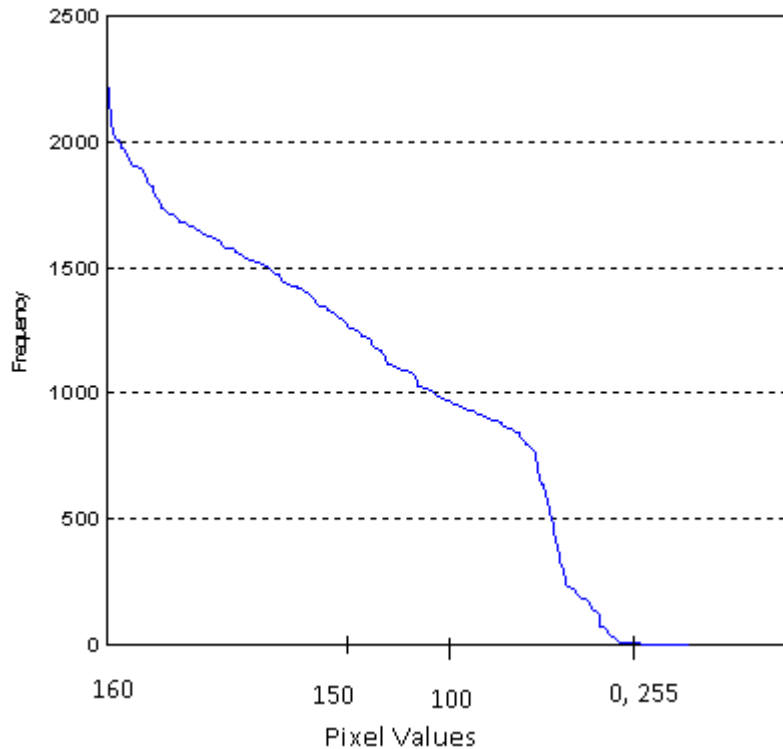
Reviewer #3: The references to be arranged in sequence, for example, on page 4 the sequence has been changed from reference 4 to 15.

The authors understand that the Neurocomputing journal requests the use of numeric references style with no emphasis on the order of the references as shown in their latest open access paper: Y. Choi, S. Ozawa, M. Lee, "Human Intention Recognition based on Eyeball Movement Pattern and Pupil Size Variation ", Neurocomputing, 2014.

However, as requested by the reviewer the order of the references has been re-arranged.

On Page 5, Figure 2, I would recommend writing proper scale for x-axis.

As Figure 2 is just a redraw of Figure 1 with the frequency decreasing rather than the pixel values. Including the pixel values in the x-axis will make the figure confusing to the readers rather than clarifying the picture. Hence we have not included the x-axis values. To illustrate this, Figure 2 will look like this:



We are certainly happy to include the x-axis in Figure2 in the final manuscript if the reviewer insists on this.

For Page 9, I would suggest to make Figure 4 clearer (i.e. the neurons structure)

The authors have made Figure 4 clearer.

In section 5.1; it has been mentioned that 10% to 20% or even the complete image is used as a training sample. If you can justify your choice here that will help other researchers.

In our experiments, we have utilised 10% to 20% or a complete image or several images combined together to look at the best number of training set used for training the image neural network predictor. Our extensive simulations indicated that there are conflicting results. The training error and the mean square error (performance indicators) improved consistently as the number of tested image rows was increased for two of the test images (Peppers.bmp and Zelda.png) and the performance indicators reduced as the number of tested image rows for the Baboon.bmp and Barbara.png test images was increased.

Hence we can't say that 10% or 20% is enough for the training the neural network predictor and therefore extensive simulations are still required for training any neural network. This explanation was added to the text of the paper for better clarification.

The results on tables 2 to 7, I would suggest to add under compressed file size for (HPWA and JPEG2000) systems (i.e Bytes) as written on the original file size column. Furthermore, that applies for table 8 and the unit for PSNR in dB.

The compressed size of the images were already added to Tables 2, 7 under heading Compressed File Size (JPEG file size + DPCM overhead) for the proposed technique and Compressed file size for the JPEG2000. For more clarity, the authors have added the bytes in parentheses. The average

image sizes were also included in Table 8 under heading Average File size and we have also included the Bytes in parentheses for clarification.


Author Agreement

I the undersigned declare that this manuscript is original, has not been published before and is not currently being considered for publication elsewhere.

I confirm that the manuscript has been read and approved by all named authors and that there are no other persons who satisfied the criteria for authorship but are not listed. I further confirm that the order of authors listed in the manuscript has been approved by all of us.

I understand that the Corresponding Author is the sole contact for the Editorial process. She is responsible for communicating with the other authors about progress, submissions of revisions and final approval of proofs.

Signed by corresponding author as follows:



(Abir Hussain)

School of Computing and Mathematical Sciences, Liverpool John Moores University

Hybrid Neural Network Predictive-Wavelet Image Compression System

Abir Jaafar Hussain^{a,*}, Dhiya Al-Jumeily^a, Naeem Radi^b and P. J.G. Lisboa^a

^aSchool of Computing and Mathematical Sciences

Liverpool John Moores University

Liverpool L3 3AF, UK

^bAl Khawarizmi University College, UAE

Abstract- This paper considers a novel image compression technique called Hybrid Predictive Wavelet coding. The new proposed technique combines the properties of predictive coding and discrete Wavelet coding. In contrast to JPEG2000, the image data values are pre-processed using predictive coding to remove inter-pixel redundancy. The error values, which are the difference between the original and the predicted values, are discrete wavelet coding transformed. In this case, a nonlinear neural network predictor is utilised in the predictive coding system. The simulation results indicated that the proposed technique can achieve good compressed images at high decomposition levels in comparison to JPEG2000.

Keywords—Neural Network, predictive coding, image compression, quantisation.

1. Introduction:

Digital image compression is a topical research area in the field of multimedia processing. Image and video compressions are essential for image transmission applications such as TV transmission, video conferencing, remote sensing via satellite (aircraft, radar or sonar) and facsimile transmission of printed materials as well as where pictures are stored in databases, such as archiving medical images, finger prints, educational and business documents and drawings. The major focus is to develop different compression schemes that provide good visual quality with fewer bits to represent digital images.

JPEG2000 Image Coding Standard was produced by the Joint Photographic Experts Group (JPEG) under the auspices of the International Standards Organization (ISO) as the successor for their earlier image coding standard JPEG. As expected,

*Corresponding author Tel.: +44(0)1512312458, Fax: +44(0)1512074594

JPEG2000 is more efficient than JPEG in terms of the compression ratio and the quality of the reconstructed image (at a fixed compression ratio) [1].

Although JPEG2000 offers a range of new and very important features, it has not used widely in some application areas such as web applications and mobile computing, where JPEG is still the most widely used standard. The reasons for this are mainly attributed to the computational complexity of the standard which makes image coding a slow process. Furthermore, the small increase in compression ratio has not seemed to convince the application developers that the benefit is enough to justify the extra computational complexity.

Several image compression techniques such as directionlets based methods [2], and hybrid methods that integrate Discrete Wavelet Transform (DWT) and fractal coding [3] or Discrete Cosine Transform (DCT) [4] are still being investigated to achieve high compression ratios without noticeable loss in the image quality. Delaunay et al. [5] suggested the use of an image compression scheme with a tuneable complexity-rate-distortion trade-off and wavelet transform. Their technique was applied for the compression of satellite images. While Bitra et al. [6] showed the criterion satisfied by an optimal transform of a JPEG2000 compatible compression scheme, using high resolution quantisation hypothesis and without the Gaussianity assumption.

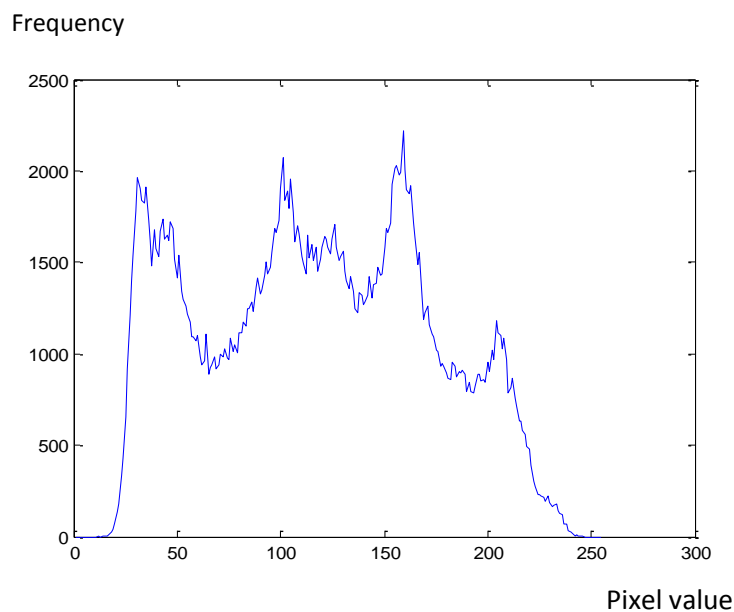


Figure 1: Frequency distribution of the pixel values of the test image Barbara.bmp (512×512)

Let us consider the frequency distribution of the pixel values of the test image Barbara which is a resolution of (512x512) pixels of grey-scale values between 0 and 255.

Figure 1 shows the frequency distribution of the pixel values. As it can be noticed, some pixel values are repeated more than others.

Generally speaking, an image that is an ideal candidate for compression should have:

1. Large amounts of data redundancy e.g. small numbers of pixel values are repeated many times while most other pixel values are repeated only few times.
2. Redundant data that is generally in large homogenous regions.

By inspecting Figure 1, it is obvious that it has relatively large amounts of data redundancy since some values are repeated more than 2000 times while other values are repeated less than 500 times. However, the graph in Figure 1 cannot be interpreted easily. Sorting the pixel values in descending order will result in the graph shown in Figure 2.

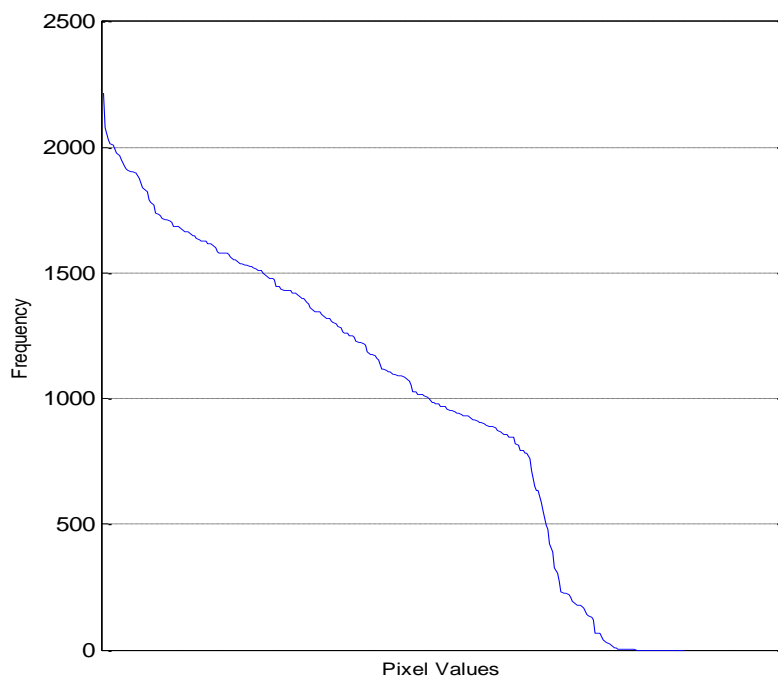


Figure 2: The frequency distribution of the pixel values of the test image Barbara.bmp (512x512) plotted in descending order

By reviewing the graph in Figure 2, it is clear that around two thirds of the pixels occurred more often than the average frequency.

In general, the effectiveness of image coding improves when the entropy of the representation reduces.

This paper proposes a novel image compression technique based on predictive coding, neural networks and DWT which we call Hybrid Neural Network Predictive Wavelet and Arithmetic (HNNPWA) image coding. In the proposed work, Differential Pulse Code Modulation (DPCM) or Predictive Coding was used to remove inter-pixel redundancy and produce Prediction Errors (PE) which has smaller entropy than the original image data. In order to improve the performance of the proposed system, the neural network is utilised as a nonlinear predictor structure.

The remainder of the paper is organised as follows. Section 2 presents the application of neural networks in image compression. Section 3 illustrates various neural network architectures that have been used in the proposed system which includes the structure of the NARX neural network and the functional link neural network. Section 4, discusses the structure of the proposed Hybrid Neural Network Predictive Wavelet Image Compression System while section 5 shows simulation results with in depth discussion. Finally, section 6 demonstrates the conclusion and direction for future works.

2. The Application of Neural Networks In Image Compression:

Dianat et al [7] used MLPs as predictor structures in DPCM. The network consists of 3 input units (the immediate causal neighbours), 30 hidden units and 1 output unit representing the predictor value. Their experiments have shown an improvement of 4 dB in the SNR, in comparison to linear prediction. He et al [8] reported similar results, while stressing the use of the quantised prediction error in the network cost function. The main disadvantages with using MLPs are long training times, complex network architecture and that there is no clear defined scheme to extract the information acquired by the network, such that it can be utilised in a similar prediction task.

Manikopoulos [9] applied higher-order predictors (a special type of functional-link networks [10]), which take into account the non-linear interactions of the input terms, thus achieving efficient input-output mappings without the need of hidden layers. In this case, the output of n -th order HONN is given by:

$$y_i^n = f\left(\sum_n T_n(i)\right) = f(T_0(i) + T_1(i) + T_2(i) + \dots + T_n(i)) \quad (1)$$

where $T_0(i)$ and $T_1(i)$ are first order terms, while $T_2(i)$ and $T_n(i)$ are given by

$$T_2(i) = \sum_k \sum_j w_{ijk} X_j X_k \quad (2nd \text{ order terms}) \quad (2)$$

$$T_n(i) = \sum_n \cdots \sum_j w_{ij \cdots n} X_j \cdots X_n \quad (n\text{-th order terms}) \quad (3)$$

In 1-D DPCM, the network was selected to be of 4th order, with 4 previous pixels as inputs and one output node. Simulation results have shown SNRs of 27.22 dB and 26.87 dB for the LENA and BABOON images, respectively. This provided an improvement in the order of 4.17dB and 3.74 dB respectively, when compared to linear DPCM. In the case of 2-D DPCM, the corresponding neural network structure was of 3rd order, with 9 previous “causal” pixel inputs and one output. The neural predictor demonstrated a SNR of 29.5 dB in the case of the LENA image.

The application of recurrent neural networks to image prediction has also been suggested. Park and Park [11] proposed the use of bilinear recurrent neural network in 2-D, DPCM; In this case an average SNR of 28.5 dB was achieved. Hussain and Liatsis [12] developed the recurrent Pi-Sigma architecture, which provides average SNRs of 29 dB and 31.6 dB, in 1-D and 2-D DPCM, respectively.

3. Neural Network Architectures Utilised in the Proposed Image Compression System:

In this section, two types of neural network architectures including the functional link network and the recurrent NARX neural network will be discussed.

3.1 Functional Link Neural Network (FLNN)

The FLNN neural network was used as the predictor structure for the proposed Hybrid Neural Network Predictive-Wavelet Image Compression System.

Functional Link Neural Network was introduced by Giles and Maxwell [13]. The network determines the product of the network inputs at the input layer, while at the output layer the summations of the weighted inputs are calculated.

FLNN can use higher order correlations of the input components to perform nonlinear mappings using only a single layer of units. Since the architecture of the network consists from a single layer, the network is aimed to reduce the computational cost in the training stage and at the same time maintaining good

approximation performance [14].

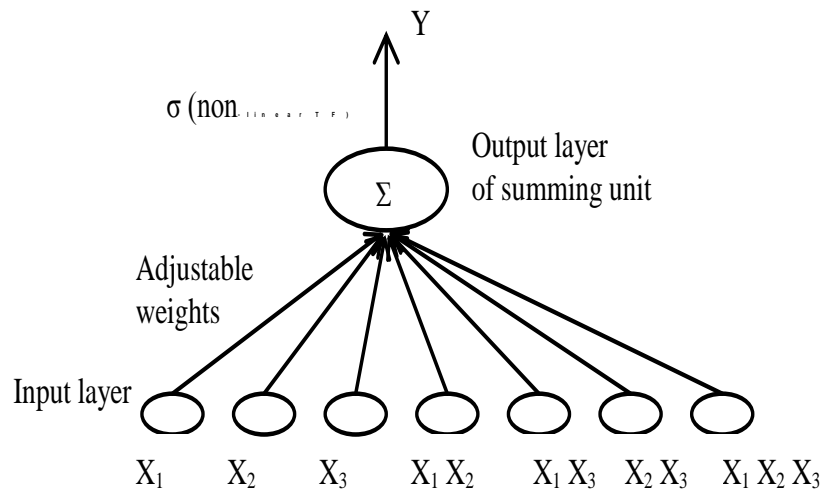


Figure 3: The Structure of the Functional Link Neural Network.

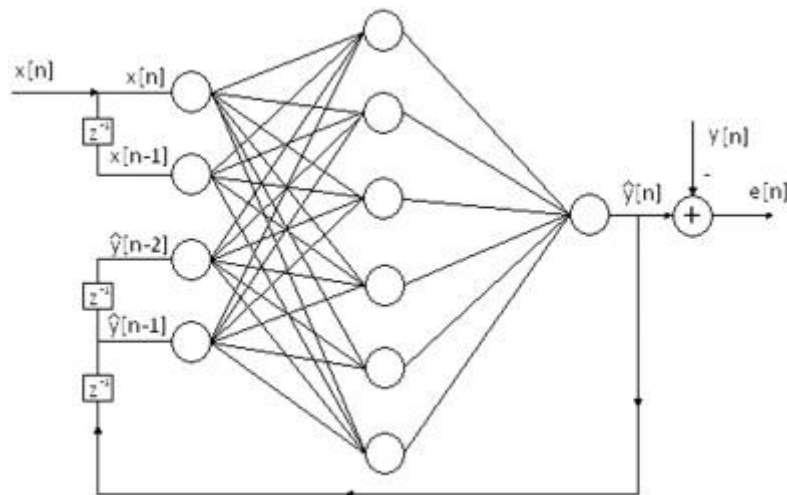


Figure 4: The structure of the NARX neural network [15].

A single node in the FLNN model could receive information from more than one node by one weighted link. The higher order weights, which connect the high order terms of the input products to the upper nodes have simulated the interaction among several weighted links. For that reason, FLNN could greatly enhance the information capacity and complex data could be learnt [14, 16,17].

Fei and Yu [18] indicated that FLNN has a powerful approximation capability in comparison to conventional Backpropagation network, and it is a good model for system identification [14]. Cass and Radl [16] used FLNN in process optimization and found that FLNN can be trained much faster than an MLP network without

scarifying computational capability. Furthermore, FLNN has the properties of invariant under geometric transformations [19]. The model has the advantage of inherent invariance, and only learns the desired signal. Figure 3 shows an example of a third order FLNN with three external inputs, x_1 , x_2 , and x_3 , and four high order input values which act as higher order input terms to the network.

The output of FLNN is determined as follows:

$$Y = f \left(W_0 + \sum_j W_j X_j + \sum_{j,k} W_{jk} X_j X_k + \sum_{j,k,l} W_{jkl} X_j X_k X_l + \dots \right) \quad (4)$$

where f is a nonlinear transfer function and W_0 is the adjustable threshold.

FLNN suffers from the computational complexity as the number of input values is increased. Hence, second or third order functional link networks are considered in practice [20-21]. Furthermore, the network is trained using the backpropogation with gradient descent algorithm, which exhibits slow convergence [22-25].

3.2 Recurrent NARX Neural Network:

This network can inherit the mapping capability of feed forward networks and meanwhile it is able to learn the dynamic features of the image information.

The nonlinear autoregressive models with exogenous inputs (NARX) recurrent neural architectures [26] have feedback connections that come from the output neuron instead of the hidden neurons. In theory, it has been shown that the NARX networks can be used, rather than conventional recurrent networks, without computational loss and that they are equivalent to Turing machines [27].

Figure 4 shows the structure of the recurrent NARX neural network.

Consider the following equation for the Nonlinear AutoRegressive with eXogenous inputs (NARX) model [12]:

$$y(t) = f(u(t-1), u(t-2), \dots, u(t-n), y(t-1), y(t-2), \dots, y(t-m), w) \quad (5)$$

In this case, $u(t)$ and $y(t)$ represent the input and the output of the network at time t , respectively. While n and m are the input-memory and output-memory order w represents the weights matrix, and the function f is a nonlinear function. In this case, the output at time t depends on both m and n past values of the input and output.

When the function f can be approximated by a multilayer perceptron (MLP), the system is defined as NARX network [26, 28].

4. The structure of the Hybrid Neural Network Predictive Wavelet Image Compression System (HNNPW):

In this section, the structure of the novel neural network based hybrid image compression system will be discussed.

The proposed system encoder consists of 3 stages. In the first stage, the FLNN neural network is utilised as predictor structure. The error signals which are the difference between the original and the predicted signals are forwarded to the second stage of the encoder. In this case, a Discrete Wavelet Transform (DWT) is utilised to transform the error signals into Wavelet coefficients. In the final stage, the transform coefficients of the most significant band will be Entropy encoded using Arithmetic Coding. Figure 5, shows the structure of the proposed HNNPWA encoder.

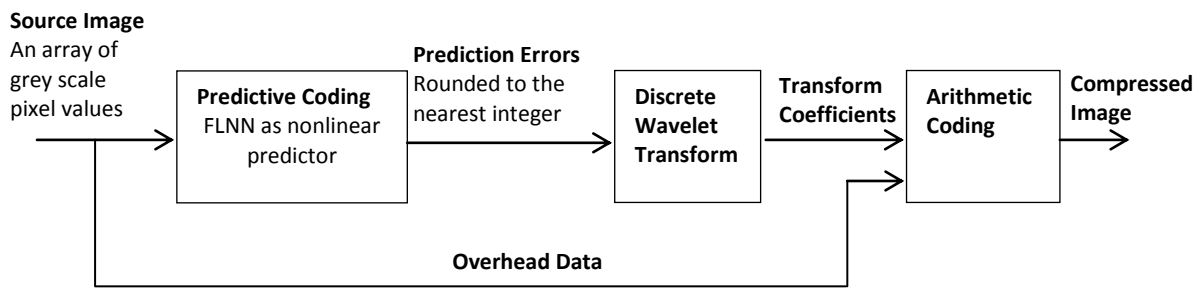


Figure 5: The encoder of the proposed neural network hybrid image compression system.

Let $S(i)$ represents the input signal (which is the image grey level in our case). In this case, $S(i)$ is forwarded to the nonlinear predictor. The predictor will use the previous encoded value to predict the current value of the signal. The difference between the predicted value and the original value is:

$$e(i) = S(i) - \hat{S}(i) \tag{6}$$

Where $\hat{S}(i)$ is the output of the neural network. For third order FLNN using 1-D DPCM with three inputs values as shown in Figure 3, the output of the network is determined as follows:

$$\hat{S}(i) = f(W_1 S(i-1) + W_2 S(i-2) + W_3 S(i-3) + W_3 S(i-1)S(i-2) + W_4 S(i-2)S(i-3) + W_5 S(i-1)S(i-2)S(i-3))$$

(7)

Where f is a nonlinear transfer function.

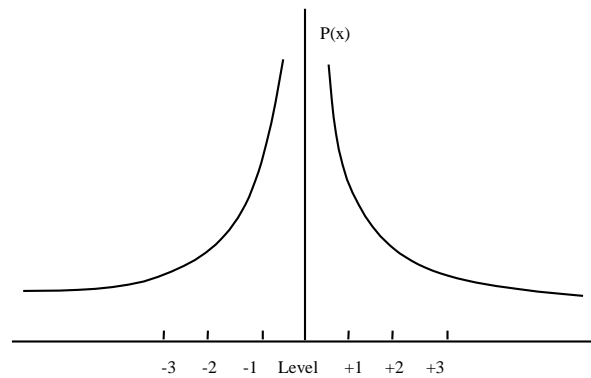


Figure 6: Schematic representation of the probability density distribution of the error sequences.

Given that the assumption of spatial causality holds, the error signal has smaller entropy than the original input signal S . Thus, the error signal is quantised with a smaller number of levels and subsequently forwarded to the DWT. This introduces an amount of quantisation error $q(i)$, such that the quantised error signal is given by:

$$e_q(i) = e(i) + q(i)$$

(8)

The error sequences can have values twice the range of the original sequences, however, the probability density function of the difference signal is a two side exponential with the structure shown in Figure 6. This means that small error values occur more frequently than large error values. The next step is to feed the quantised prediction error array e_q to the DWT module. The DWT technique is fairly simple, the 1-D time-amplitude signal (the error image data) is decomposed into high frequency band and low frequency band by passing the signal through low pass and high pass filters respectively (level 1). This process is repeated by decomposing the low frequency band into low-low and low-high frequency bands and also decomposing the high frequency band into high-low and high-high frequency bands (level 2). The process may be repeated several times (level 3 and deeper levels).

Figure 7 shows how the two dimensional array is divided after each level in sub-band coding. Therefore, after decomposition level 3, the most significant data (transform

coefficients of the error signal) will be in LL₃. The data (transform coefficients of the error signal) in all other sub-arrays can be ignored and a zero will be assumed for their values by the inverse DWT algorithm at the decoder.

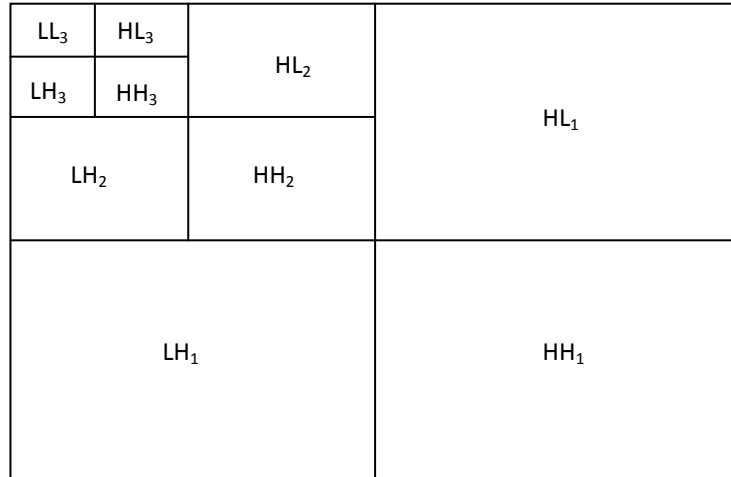


Figure 7: The dyadic decomposition of an array into frequency sub-bands.

HL: High frequency band with Low pass filters
 HH: High frequency band with High pass filters
 LL: Low frequency band with Low pass filters
 LH: Low frequency band with High pass filters

5. Simulation Results:

We have carried out two sets of experiments. In the first set of experiments, the aim is to determine a suitable neural network structure that can be used in the proposed image compression system, as well as the most suitable image that can be used in the training process of the neural network and the structure of the input combinations from the image data.

TABLE 1: six test images, their sizes and the range of maximum and minimum values in each image.

#	Test Image	Image Size	Minimum Value	Maximum Value
1	Baboon	512×512	0	230
2	Barbara	512×512	8	36
3	Cameraman	256×256	7	253
4	Lena	512×512	8	35
5	Peppers	512×512	0	229
6	Zelda	512×512	0	187

In the second set of experiments, the information provided from the first set of experiments will be utilised for building the proposed neural network hybrid system. Six test images as shown in Table 1 were coded by the proposed HNNPWA system and then by JPEG2000 at decomposition levels 1 to 6.

The performance of these schemes is characterised using different image quality metrics including the MSE, the mean absolute value and the Peak Signal to Noise Ratio (PSNR) as image quality metrics based error.

The PSNR is defined as follows:

$$PSNR = 10 \log_{10} ((255)^2 / MSE) \quad (9)$$

where MSE is the mean square of the error between the original and the reconstructed images, and it is defined as:

$$MSE = \frac{1}{MN} \sum_{i=1}^M \sum_{j=1}^N (x_{ij} - y_{ij})^2 \quad (10)$$

where MN is the total number of pixels in the image.

The Mean absolute value of the error is determined as follows:

$$MAE = \frac{1}{MN} \sum_{i=1}^M \sum_{j=1}^N |x_{ij} - y_{ij}| \quad (11)$$

5.1 First set of experiments:

Test images such as Barbara and Lena are used extensively by almost all researchers in the field of still image compression. These test images were chosen because each image has certain feature which constitutes a challenge for the prediction algorithm used in image coding, for example, Barbara has many dark and light stripes and various edges which are difficult to predict. While the Lena image, which is one of the most popular images used in image processing, contains moderate amount of detail. It is characterised by strong edges defined by the head and the shoulder.

These test images were initially selected for use with hard prediction algorithms (mathematical algorithms) rather than in soft prediction algorithms (neural prediction algorithms), as some of these images are not suitable for neural image prediction.

The neural network is usually trained using part of an image (10% to 20%) or a complete image or several images combined together.

In our experiments, the Peppers.bmp was first selected and used as test image for the neural predictive system. The number of rows used during the training was selected between 20, 40, 60, 100 and 200 rows. The training error and the mean square error were noted in each case.

The same experiment was repeated for three other test images which are the Baboon.bmp, Zelda.png and Barbara.png test images

The simulation results showed conflicting results. The training error and the mean square error (performance indicators) improved consistently as the number of tested image rows was increased for two of the test images (Peppers.bmp and Zelda.png) and the performance indicators reduced as the number of tested image rows for the Baboon.bmp and Barbara.png test images was increased. This indicates that when using neural network predictors for image compression, extensive simulations are required to train the neural network predictors.

Then three test images Peppers.bmp, Zelda.png and Barbara.png combined together in one image file to train the same neural predictive system. Our simulation results indicated that the performance indicators in this case were poorer than all previous cases.

The results indicate that marginal improvements can be achieved if large number of rows is used to train the neural predictive systems for some of the test images. Furthermore, combining several test images together in order to train the network does not guarantee good performance.

All test images used in this experiment are grey level images with the extension of 'bmp' or 'png', hence pixel values range between 0 and 255. As it can be noticed from Table 1, the ranges for the maximum and minimum data values for the Lena and the Barbara images are relatively small (around 30) whereas the pixel value ranges for the remaining images are relatively large and covers large range of the grey level.

The simulation results showed that for hard predictive coding algorithms that use fixed (hard) mathematical formulas to predict the next value, using any test images with small or large pixel ranges does not affect the performance of the predictors. However, our experiments indicated that images with large number of grey level ranges showed much better performance in terms of the MSE than the Barbara and the Lena images when used to train neural predictive coding system.

(a)

X1	X2	X3	X4	X5	X6	X7	X8	P		

(b)

								X5		
							X3	X4	X6	
						X1	X2	P		

(c)

								X6		
						X3	X4	X5	X7	X8
						X1	X2	P		

Figure 5: P = pixel to be predicted, Xi are the input values for the neural prediction system, (a), (b) and (c) are three possible schemes for selecting the input values for the network.

Furthermore, we have investigated the effect of choosing several schemes for input values on the performance of the neural prediction system as shown in Figure 5.

In this case, three types of experiments were performed. In the first type of experiments as shown in Figure 5 (a), 8 previous pixels values to the left of the current pixel on the same row are used as inputs to the neural network system, the same experiments were repeated for 4 and then 2 previous pixel values. No improvements were noted by reducing the number of pixels from 8 to 4, however, the performance of the system dropped when we reduced the number of pixels from 4 to 2 previous pixel values.

In the second type of experiments as shown in Figure 5 (b), 2 pixels from the left, 2 pixels from the upper left corner, 2 pixels above and 2 pixels from the upper right corner of the current pixel have been used as input values to the neural network, better simulation results were obtained in terms of PSNR.

In the final type of experiments, the same inputs are used with one additional input from the left upper corner and one additional input from the right upper corner as shown in Figure 5 (c). The simulation results indicated that there were no major improvements in the PSNR when compared with the results obtained from the previous scheme.

In conclusion, the choice of the test image that will be used for training and testing the neural predictive coding system, as well as the size of the training and test samples are all very important factors that determine the success of the neural network predictor.

Various neural network architectures including the Multi-Layer Perceptron (MLP), Polynomial and recurrent NARX Neural Networks have been designed and tested to model the behaviour of nonlinear predictor. We have also tested linear predictor for comparison reasons.

The simulation results indicated that the average MSE and PSNR for the test images are 146.8 and 28.19 respectively using the MLP network, which gives the nonlinear MLP predictor an average improvement of 2.22 dB over the linear predictor.

The average MSE and PSNR for the test images are 139.2 and 28.59 dB, respectively using the FLNN predictor. This is an improved result when compared with the MLP predictor structure.

Finally, the simulation results for the NARX predictor structure indicated that the average MSE and PSNR for the test images are 245.8 and 25.97, respectively.

These results indicated that the FLNN has achieved better results in comparison with the NARX and the MLP predictors. Hence, a functional link neural network predictor was utilised in the proposed HNNPWA image compression system.

It is worth mentioning that Billings et al. [29] demonstrated that neural network does not generate components of lagged system inputs and outputs that are not specified in the inputs nodes and that if insufficiently and inappropriately lagged values for the inputs and the previous outputs are assigned as input signals, the network cannot generate the missing dynamic terms. This illustrate that the network does not “learn” the system behaviour completely and it will not be a general model of the system, and hence the network performance will be limited. As a result, there should be a trade-off of between the number of inputs and higher order terms passed to the FLNN neural network to generate good prediction when used as a predictor structure in the proposed system.

5.2 Second set of experiments:

In the second set of experiments, the proposed system was utilised for the compression of the grey level images shown in Table1. The discrete wavelet transform was looked at with the decomposition levels were tested from 1 to 6 and the results are tabulated in Tables 2 to 7.

In terms of the compressed signal quality (MSE and PSNR), the JPEG2000 system performs better than the HNNPWA system at decomposition levels 1 and 2. It can be noted that JPEG2000 achieved better performance at these levels due to the type of redundancy (inter-pixel redundancy) that exists in the original image data. However, starting from level 3 and above, the HNNPWA system starts to perform better and the difference becomes greater as we move to higher decomposition levels.

TABLE 2: Functional link network trained on test image peppers DWT level 1 (2 bpp or compression ratio of 4:1).

#	Test Image (bmp)	Original File Size (Bytes)	HNNPWA System					JPEG2000 System			
			MSE	MAE	PSNR	Compressed File Size (Bytes) (JPEG file size + DPCM overhead)	File	MSE	MAE	PSNR	Compressed File Size (Bytes)
1	Baboon	263,222	290	11.80	23.53	65,423	1,483	22	1.80	34.83	65,423
2	Barbara	263,222	207	7.75	25.99	65,374	1,573	3	0.66	43.14	65,374
3	Cameraman	66,614	153	6.12	26.30	16,314	663	3	0.58	44.00	16,314
4	Lena	263,222	38	4.51	32.36	65,411	863	4	0.75	42.12	65,411
5	Peppers	263,222	35	4.06	32.62	65,508	1,500	3	0.66	43.16	65,508
6	Zelda	263,222	12	2.68	37.04	65,404	1,406	1	0.41	46.68	65,404
	Average		122.5	6.15	29.64	57,239	1,248	6	0.81	42.32	57,239

TABLE 3: Functional link network trained on test image peppers DWT level 2 (0.5 bpp or compression ratio of 16:1).

#	Test Image (bmp)	Original File Size (Bytes)	HNNPWA System				JPEG2000 System				
			MSE	MAE	PSNR	Compressed File Size (Bytes) (JPEG file size + DPCM overhead)	MSE	MAE	PSNR	Compressed File Size (Bytes)	
1	Baboon	263,222	396	13.75	22.95	16,163	1,483	182	5.04	25.55	16,163
2	Barbara	263,222	249	8.88	25.22	16,156	1,573	39	2.28	32.20	16,156
3	Cameraman	66,614	202	7.05	26.01	4,021	663	53	2.36	30.95	4,021
4	Lena	263,222	51	5.11	32.05	16,378	863	19	1.69	35.31	16,378
5	Peppers	263,222	49	4.62	32.20	16,378	1,500	17	1.53	35.94	16,378
6	Zelda	263,222	16	2.98	36.35	16,071	1,406	7	1.08	39.62	16,071
	Average		160.5	7.06	29.13	14,194	1,248	52.83	2.33	33.26	14,194

TABLE 4: Functional link network trained on test image peppers, DWT level 3 (0.125 bpp or compression ratio of 64:1).

#	Test Image (bmp)	Original File Size (Bytes)	HNNPWA System				JPEG2000 System				
			MSE	MAE	PSNR	Compressed File Size (Bytes) (JPEG file size + DPCM overhead)	MSE	MAE	PSNR	Compressed File Size (Bytes)	
1	Baboon	263,222	405	14.05	22.55	3,901	1,483	453	7.74	21.60	3,901
2	Barbara	263,222	245	9.14	24.82	3,943	1,573	199	4.83	29.27	3,943
3	Cameraman	66,614	210	7.26	25.68	1,020	663	248	4.78	24.22	1,020
4	Lena	263,222	53	5.29	31.15	4,090	863	60	2.76	30.40	4,090
5	Peppers	263,222	54	4.82	31.10	4,036	1,500	57	2.59	30.60	4,036
6	Zelda	263,222	17	3.11	35.95	4,079	1,406	22	1.69	34.77	4,079
	Average		164	7.28	28.54	3,511	1,248	173.17	4.07	28.48	3,511

Table 8 shows the average performance of the proposed HNNPWA and JPEG2000 achieved at each decomposition levels using the MSE, the MAE and the PSNR.

As can be seen from Table 8, the average MSE values for the HNNPWA system are 9.17, 332, 2654 and 2,330 better than the JPEG2000 system at decomposition levels 3, 4, 5 and 6, respectively. Furthermore, Table 8 indicated that the average PSNR value for the HNNPWA system is 0.06 dB, 5.05 dB, 13.75 dB and 11.26 dB better than the JPEG2000 at decomposition levels 3, 4, 5 and 6, respectively. Using the MAE, the simulation results indicated an average improvement of 7.41 and 7.84 at decomposition levels 5 and 6 respectively.

A paired t-test [30] is conducted to determine if there is any significant difference among the proposed HNNPWA and JPEG2000 image compression techniques based on the MAE of the error image. The calculated t-value showed that the proposed technique outperform JPEG2000 with $\alpha = 5\%$ significance level for a one-tailed test at decomposition levels 4, 5 and 6. The t-test indicated that there is no significant difference between the two image compression techniques at decomposition level 3.

TABLE 5: Functional link network trained on test image peppers, DWT level 4 (0.03125 bpp or compression ratio of 256:1).

#	Test Image	Original File Size	HNNPWA System				JPEG2000 System				
			MSE	MAE	PSNR	Compressed File Size (Bytes) (JPEG file size + DPCM overhead)	MSE	MAE	PSNR	Compressed File Size (Bytes)	
1	Baboon	263,222	418	14.07	21.95	974	1,483	663	9.32	19.95	974
2	Barbara	263,222	257	9.26	24.05	1,025	1,573	430	7.32	21.83	1,025
3	Cameraman	66,614	220	7.37	24.74	253	663	1,387	11.30	16.74	253
4	Lena	263,222	58	5.38	30.46	996	863	203	4.95	25.08	996
5	Peppers	263,222	59	4.93	30.39	1,024	1,500	255	5.20	24.09	1,024
6	Zelda	263,222	19	3.19	35.25	998	1,406	85	3.17	28.86	998
	Average		171.83	7.36	27.81	878	1,248	503.83	6.88	22.76	878

TABLE 6: Functional link network trained on test image peppers DWT level 5 (0.0078 bpp or compression ratio of 1024:1).

#	Test Image	Original File Size	HNNPWA System				JPEG2000 System				
			MSE	MAE	PSNR	Compressed File Size (Bytes) (JPEG file size + DPCM overhead)	MSE	MAE	PSNR	Compressed File Size (Bytes)	
1	Baboon	263,222	425	14.08	21.94	248	1,483	1,473	17.3	16.48	248
2	Barbara	263,222	261	9.37	24.02	231	1,573	3,094	18.15	13.25	231
3	Cameraman	66,614	224	7.41	24.70	231	663	3,972	20.67	12.17	231
4	Lena	263,222	62	5.45	30.38	253	863	1,584	15.34	16.16	253
5	Peppers	263,222	64	5.06	30.21	231	1,500	3,861	14.28	12.29	231
6	Zelda	263,222	22	3.31	35.00	231	1,406	2,998	3.37	13.39	231
	Average		176	7.44	27.71	237	1,248	2,830.3	14.85	13.96	237

TABLE 7: Functional link network trained on test image peppers DWT level 6 (0.00195 bpp or compression ratio of 4096:1).

#	Test Image	Original File Size	HNNPWA System				JPEG2000 System				
			MSE	MAE	PSNR	Compressed File Size (Bytes) (JPEG file size + DPCM overhead)	MSE	MAE	PSNR	Compressed File Size (Bytes)	
1	Baboon	263,222	725	14.11	19.93	248	1,483	1790	18.04	15.63	248
2	Barbara	263,222	880	9.45	21.00	231	1,573	3,190	18.15	12.25	231
3	Cameraman	66,614	824	7.65	21.66	231	663	3,972	20.67	12.17	231
4	Lena	263,222	590	5.50	27.33	253	863	2,312	17.86	14.52	253
5	Peppers	263,222	684	5.19	27.08	231	1,500	3,861	14.21	12.29	231
6	Zelda	263,222	441	3.38	30.85	231	1,406	2,998	3.37	13.39	231
	Average		690	7.54	24.64	237	1,248	3,020.5	15.38	13.38	237

TABLE 8: The average MSE and PSNR values for the HPWA and JPEG2000 systems.

Decomposition Level	HNNPWA				JPEG200			
	Average MSE	Average MAE	Average PSNR	Average File Size (Bytes)	Average MSE	Average MAE	Average PSNR	Average File Size (Bytes)
1	122	6.15	29.64	58,487	6	0.81	42.32	56,708
2	160	7.06	29.13	15,885	52	2.33	33.26	14,104
3	164	7.28	28.54	5,280	173	4.07	28.48	3,499
4	171	7.36	27.81	2,647	503	6.88	22.76	866
5	176	7.44	27.71	2,023	2,830	14.85	13.96	242
6	690	7.54	24.64	1485	3,020	15.38	13.38	237

As can be seen from Figure 8, at decomposition levels 1, 2 and 3, the visual quality of the reconstructed images for the proposed HPNWA and JPEG2000 is very good

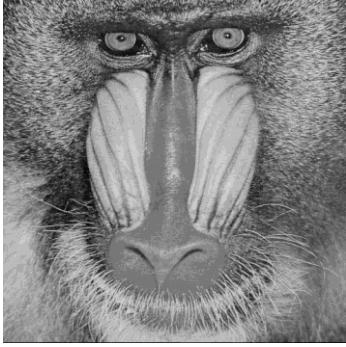
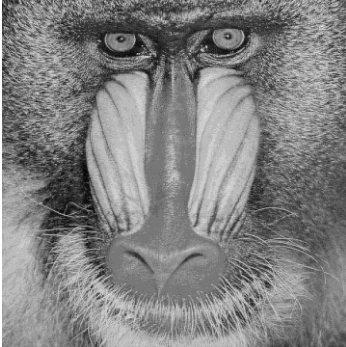
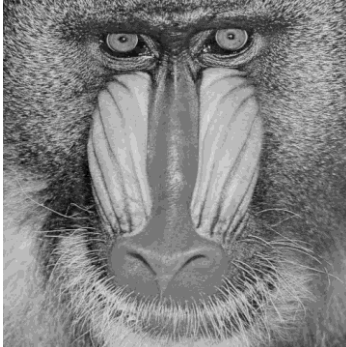
and it is not easy to notice the difference between the original image and the constructed image for both systems.

While at decomposition level 4 and 5 as shown in Figures 9(a) and 9(b), respectively, the visual quality of the reconstructed images in the JPEG2000 system starts to deteriorate. The visual quality of most reconstructed images for the JPEG2000 system is not acceptable. However, for the HNNPWA system, all reconstructed images are of a very good quality and cannot be distinguished from the original.

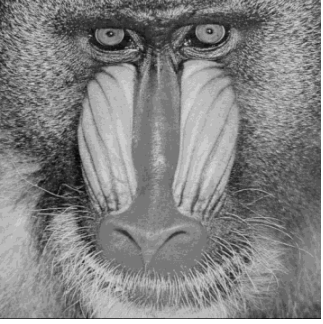
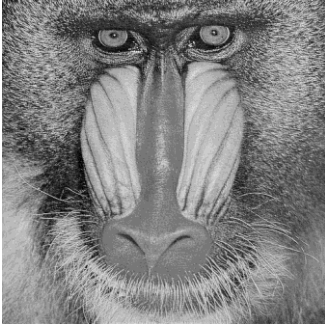
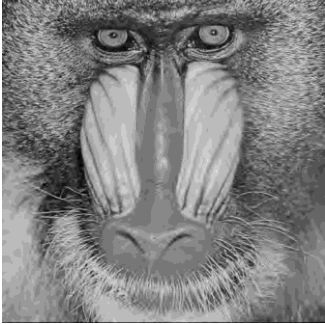
Figure 9(c) demonstrated that the Baboon image compressed at decomposition level 6. In this case, the visual quality of all reconstructed images for the JPEG2000 system is not acceptable. Furthermore, for the HNNPWA system, the quality of the reconstructed images deteriorates to an unacceptable level. This is attributed to the size of the transform coefficients array which becomes too small to hold accurate information about the prediction errors.

It should be noted that the average compressed file size in JPEG2000 system is smaller at all decomposition levels in comparison to the proposed system due to the additional fixed overhead data that has to be stored as a result of introducing Predictive Coding. However, the MSE and PSNR values as well as the visual quality for the HNNPWA system at both decomposition levels 4 and 5 are better than level 3 of JPEG2000.

(a) The visual quality of the Baboon test image compressed by the HPWA and JPEG2000 systems (DWT Compression Ratio 4: 1)

Original (bmp) image	HPWA compressed image	JPEG2000 (j2c) compressed image
		

(b) The visual quality of the Baboon test image compressed by the HPWA and JPEG2000 systems (DWT Compression Ratio 16: 1)

Original (bmp) image	HPWA compressed image	JPEG2000 (j2c) compressed image
		

(c) The visual quality of the Baboon test image compressed by the HPWA and JPEG2000 systems (DWT Compression Ratio 64:1)

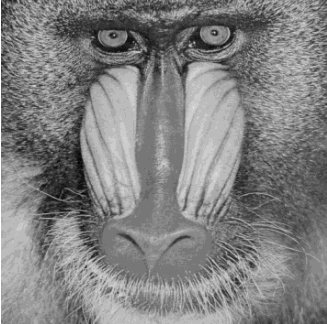
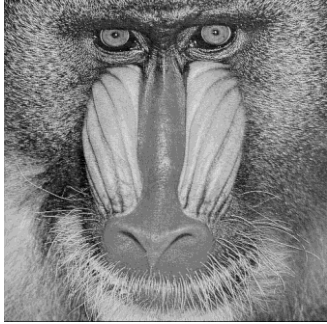

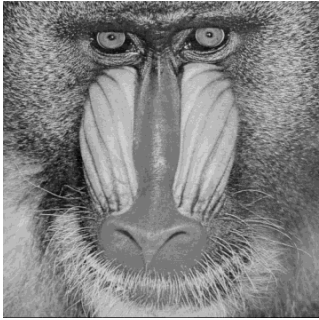
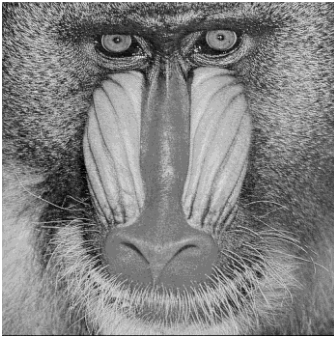
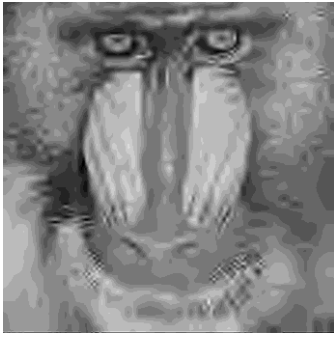
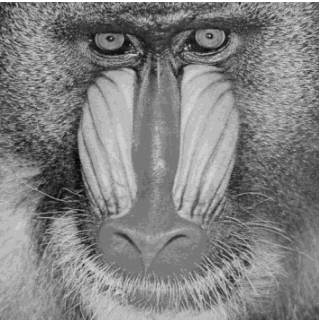
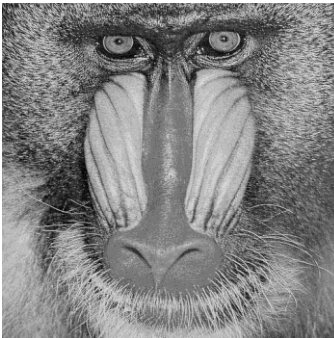
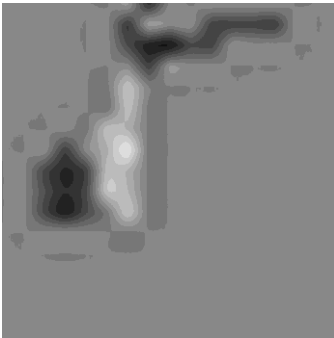
Original (bmp) image	HPWA compresses image	JPEG2000 (j2c) compress image
		

Figure 8: The visual quality of the Baboon test image compressed by the HPWA and JPEG2000 systems at decomposition level (a) 1, (b) 2 and (c) 3.

(a) The visual quality of the six test images compresses by the HPWA and JPEG2000 system (DWT Compression Ratio 256:1)

Original (bmp) image	HPWA compressed image	JPEG2000 (j2c) compressed image
		

(b) The visual quality of the six test images compresses by the HPWA and JPEG2000 system (DWT Compression Ratio 1024:1)

Original (bmp) image	HPWA compressed image	JPEG2000 (j2c) compressed image
		

(c) The visual quality of the six test images compresses by the HPWA and JPEG2000 system (DWT Compression Ratio 4096:1)

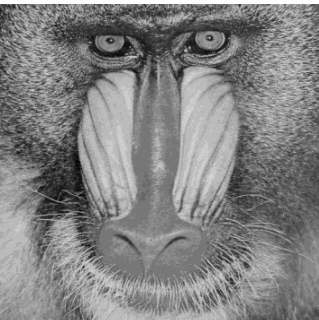
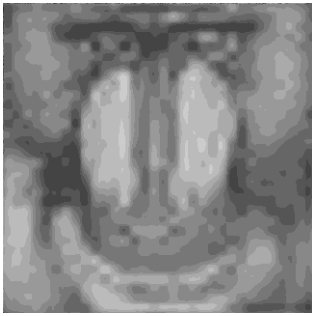

Original (bmp) image	HPWA compressed image	JPEG2000 (j2c) compressed image
		

Figure 9: The visual quality of the Baboon test image compressed by the HPWA and JPEG2000 systems at decomposition level (a) 4, (b) 5 and (c) 6.

6. Conclusion and Future works:

In this paper, a novel still image compression technique based on predictive coding transform coding, and neural network is proposed. The prediction errors produced in the first part of the proposed system are fed into the second part of the proposed

system that is Discrete Wavelet Transform. The main compression is achieved at the second part which is greatly aided by the removal of inter-pixel redundancy in due to the used of prediction coding. The transform coefficients for all but the lowest frequency bands will be nearly zero and can be dropped out without any significant loss in image quality

Simulation were carried out for the HNNPWA system and benched marked against JPEG2000 which is the still image coding standard. The results were most encouraging and have indicated a significant improvement over JPEG2000 at high compression ratios (64:1 and higher) as well as large size images. At a compression ratio of 1024:1 the reconstructed images of JPEG2000 became completely unrecognised, while the HNNPWA reconstructed images were still of a high visual quality and even better than the images compressed by JPEG2000 at compression ratio 64:1. The paired t-test was performed on the MAE of the error which indicated that the proposed HNNPWA is significantly better than JPEG2000 at decomposition 4, 5 and 6. This means that at high decomposition levels using discrete wavelet transform, the proposed system showed high quality compressed images, while at low decomposition levels the visual quality of the compressed images using the proposed technique show similar quality to JPEG2000.

As the proposed system requires the use of both predictive and transform coding in its structure, this means that this the HNNPWA requires more processing time than JPEG2000.

Future work will involve the use of other types of neural network structures such as the support vector machine [31] and dynamic ridge polynomial neural network [32].

Another direction of research is to use DWT, followed by neural network predictive coding system similar to reference [33]. This will allow the system to remove inter-pixel redundancy from the transformed image coefficients.

References

- [1] D. S. Taubman and M. W. Marcellin, "JPEG2000: Standard for Interactive Imaging", Proceedings of the IEEE, VOL. 90, NO. 8, 2002.
- [2] V. Velisavljevic, B. Beferull-Lozano, M. Vetterli "Space-frequency quantization for image compression with directionlets", IEEE Transactions on Image Processing, 16 (7), 2007, pp. 1761–1773.

- [3] Y. Iano, F.S. da Silva, A.L.M. Cru, "A fast and efficient hybrid fractal-wavelet image coder", *IEEE Transaction on Image Processing*, 15 (1) (2006), pp. 98–105
- [4] E. Elharar, A. Stern, O. Hadar, B. Javidi, "A hybrid compression method for integral images using discrete wavelet transform and discrete cosine transform" *Journal of Display Technology*, 3 (3) (2007), pp. 321–325
- [5] X. Delaunay, M. Chabert, V. Charvillat, and G. Morin, "Satellite image compression by post transform in the wavelet domain" *Signal Processing*, 90(2), 2010, pp. 599-610.
- [6] I. Bitá, M. Barret, D.T. Pham, "On optimal transforms in lossy compression of multicomponent images with JPEG2000" *Signal Processing*, 90(3), 2010, pp. 759-773.
- [7] S. A. Dianat, N. M. Nasrabadi and S. Venkataraman, "A non-linear predictor for differential pulse-code encoder (DPCM) using artificial neural networks", *International Conference on Acoustics, Speech, and Signal Processing*, 1991. ICASSP-91, Pages: 2793 - 2796 vol.4.
- [8] Z. He and H. Li, "Non-linear predictive image coding with a neural network", *Proc. ICASSP*, pp. 1009-1012, (1990).
- [9] C. N. Manikopoulos, J. Li, and H. Sun, Nonlinear neural prediction in 1D DPCM for efficient image data coding, *Acoustics, Speech, and Signal Processing*, 1991. ICASSP-91., 1991 International Conference on 14-17 Apr 1991, Pages: 3709 - 3711 vol.5.
- [10] Y.H. Pao and Y. Takefuji, "Functional-link net computing: theory, system architecture and functionalities", *IEEE Computer*, 25/5, pp. 76-79, (1992).
- [11] D-C. Park and T-H Park, "DPCM with a recurrent neural network predictor for image compression", *Proc. IEEE Conf. Neural Networks*, Vol. 2, Anchorage, AK, May 4-9, 1998.
- [12] A. J. Hussain, and P. Liatsis, "Recurrent Pi-Sigma neural network for DPCM image coding," *Neurocomputing*, vol. 55, 2003, pp.363-382.

- [13] C. L. Giles and T. Maxwell, "Learning, invariance and generalization in high-order neural networks," in *Applied Optics*, vol. 26, no. 23, Optical Society of America, Washington D. C., (1987), pp. 4972-4978.
- [14] L. Mirea, and T. Marcu "System identification using Functional-Link Neural Networks with dynamic structure," 15th Triennial World Congress, Barcelona, 2002, Spain.
- [15] E. Irigoyen and G. Miñano "A NARX neural network model for enhancing cardiovascular rehabilitation therapies", *Neurocomputing*, 109(3), pp. 9-15, 2013.
- [16] R. Cass, and B. Radl, "Adaptive process optimization using Functional-Link Networks and Evolutionary Algorithm," *Control Eng. Practice*, Vol. 4, No. 11, 1996, pp. 1579-1584.
- [17] C. L.O. Giles, R. D. Griffin, and t. maxwell, "Encoding Geometric Invariances in HONN," *American Institute of Physics*, 1998, pp. 310-309.
- [18] Fei, G., and Yu, Y. L.: 'A modified Sigma-Pi BP Network with Self-feedback and its Application in Time Series Analysis,' *Proceedings of the 5th International Conference*, vol. 2243-508F, 1994, pp. 508-515.
- [19] R. Durbin and D. E. Rumelhart, "Product Units: A Computationally Powerful and Biologically Plausible Extension to Back-propagation Networks," *Neural Computation*, vol. 1, 1989, pp. 133-142.
- [20] T. Kaita, S. Tomita, and J. Yamanaka, "On a Higher-order Neural Network for distortion invariant pattern recognition," *Pattern Recognition Letters* 23, 2002, pp 977-984.
- [21] G. Thimm, "Optimization of High Order perceptron," *Swiss federal Institute of Technology (EPFL)*, 1995.
- [22] D.S.Huang, Horace H.S.Ip and Zheru Chi, "A neural root finder of polynomials based on root moments," *Neural Computation*, vol.16, no.8, pp.1721-1762, 2004.
- [23] D.S.Huang, "A constructive approach for finding arbitrary roots of polynomials by neural networks," *IEEE Transactions on Neural Networks*, vol.15, no.2, pp.477-491, 2004.
- [24] D.S.Huang, Horace H.S.Ip, Zheru Chi and H.S.Wong, "Dilation method for finding close roots of polynomials based on constrained learning neural networks," *Physics Letters A*, vol.309, no.5-6, pp.443-451, 2003.

- [25] D.S.Huang, "Radial basis probabilistic neural networks: Model and application," *International Journal of Pattern Recognition and Artificial Intelligence*, 13(7), pp.1083-1101, 1999.
- [26] S. Chen, S. A. Billings, and P. M. Grant, "Non-linear system identification using neural networks," *International Journal of Control*, vol. 51, no. 6, 1990, pp. 1191–1214.
- [27] H. T. Siegelmann, B. G. Horne, and C. L. Giles, "Computational capabilities of recurrent narx neural networks," *IEEE Transactions on Systems, Man and Cybernetic*, pt. B, vol. 27, Apr. 1997, p. 208.
- [28] K. Narendra and K. Parthasarathy, "Identification and Control of Dynamical Systems using Neural Networks", *IEEE Transactions on Neural Networks*, Mar. 1990, 1(1), pp.4-27.
- [29] S. A. Billings, H. B. Jamaluddin, and S. Chen, "Properties of neural networks with applications to modeling non-linear dynamical systems", *International Journal of Control*, 55, (1992), 193–224.
- [30] D. C. Montgomery and G. C. Runger, *Applied Statistics and Probability for Engineers*. New York: Wiley, 1999.
- [31] Z. Shaohua, W. Yan. Suppliers evaluation of support vector machine model and its application. *Journal of Chongqing Normal University*, 2007, 24 (1), 29-33.
- [32] R. Ghazali, A. J. Hussain, N. M. Nawawi and B. Mohamad, "Non-stationary and stationary prediction of financial time series using dynamic ridge polynomial neural network," *Neurocomputing*, Volume 72, Issues 10-12, 2009, Pages 2359-2367.
- [33] D. U. Shah and C. H. Vithlani, "FPGA Realization of DA-Based 2D-Discrete Wavelet Transform for the Proposed Image Compression Approach" *Nirma University International Conference on Engineering*, 2011.

Dr. Abir Jaafar Hussain is a senior lecturer at the School of Computing and Mathematical Sciences at Liverpool John Moores University, UK. She completed her PhD study at The University of Manchester, UK in 2000 with a thesis title Polynomial Neural Networks for Image and Signal Processing. She has published numerous referred research papers in conferences and Journal in the research areas of Neural Networks, Signal Prediction, Telecommunication Fraud Detection and Image Compression. She is a PhD supervisor and an external examiner for research degrees including PhD and MPhil.

Dr. Dhiya Al-Jumeily is a principle lecturer in eSystems Engineering and leads the Applied Computing Research Group at the faculty of Technology and Environment. He has already developed fully online MSC and BSc programmes and currently heads the enterprise activities at the School of Computing and Mathematical Sciences. Dr. Al-Jumeily has published numerous referred research papers in multidisciplinary research areas including: Technology Enhanced Learning, Applied Artificial Intelligence, Neural Networks, Signal Prediction, Telecommunication Fraud Detection and Image Compression. He is a PhD supervisor and an external examiner for the degree of PhD. He has been actively involved as a member of editorial board and review committee for a number peer reviewed international journals, and is on program committee or as a general chair for a number of international conferences.

Dr. Naeem Radi is the CEO of the Al Khawarizmi University College in the UAE. His main area of research involves the design of image processing algorithms for image compression. Dr Radi has published many journal and conference papers and reports on many aspects of this research and has also acted as Session Chair and on program committees for many international conferences. He serves as professional fellowship for BCS and as a Professional Member for IEEE.

Prof. Lisboa Paulo was appointed to the chair of Industrial Mathematics at Liverpool John Moores University in 1996 where he heads the Department of Mathematics and Statistics and the Statistics & Neural Computation Research Group. He holds cross-Faculty positions as institutional link in the R&D Executive of the Royal Liverpool and Broadgreen University Hospitals NHS Trust and as Research Professor in the St. Helen's and Knowsley Teaching Hospitals NHS Trust. He is a visiting professor in the Centre for Public Health, chairs the steering committee of the Centre for Health and Social Care Informatics and co-leads the Medicine and Therapeutics network in the Institute for Health Research. He has over 200-refereed publications and four edited books.

*Photo of the author(s)
[Click here to download Photo of the author\(s\): Photos.docx](#)

